PERGAMON

International Journal of Heat and Mass Transfer 41 (1998) 3229–3238

International Journal of
HEAT and MASS
TRANSFER

Adsorption of toluene on activated carbon in a packed bed

Jung-Yang San*, Yuh-Ching Hsu, Liang-Jen Wu

Department of Mechanical Engineering, National Chung-Hsing University, 250 KuoKuang Road, Taichung 40227, Taiwan, Republic of China

Received 20 December 1996; in final form 9 January 1998

Abstract

A simulation of the performance of an activated carbon packed-bed system for adsorption of toluene from air is performed. For a non-switched operation the time-varying exit toluene concentration of a 30 mm-depth bed is measured. The simulation result is compared with the measured data. The computer analysis is based on a modified solid-side resistance model which was originally proposed by Pesaran and Mills. The effects of cycle operating time, regeneration temperature and Ntu on the adsorption performance are investigated. The maximum removal and the corresponding optimum cycle time are obtained. The influence of the number of grid points on the accuracy of the numerical scheme is discussed. The effects of tortuosity factor and transfer coefficients on the adsorption are investigated.

Key words: Packed bed; Activated carbon; Tortuosity; Adsorption; Toluene

Nomenclature

A	cross-sectional area of bed [m^2]
A_s	bed total heat or mass transfer area [m^2]
Bi_m	mass transfer Biot number, $K_G R/\rho_P D_{s,eff}$
c	specific heat [kJ kg^{-1} K^{-1}]
$c_{p,e}$	constant pressure specific heat of toluene-air mixture [kJ kg^{-1} K^{-1}]
$c_{p,l}$	constant pressure specific heat of toluene [kJ kg^{-1} K^{-1}]
C^*	mass ratio of activated carbon to processed air in adsorption, $\rho_b AL/m_G\tau$
D^*	non-dimensional surface mass diffusion parameter, $D_{s,eff}\tau/R^2$
$D_{s,eff}$	effective surface mass diffusion coefficient [m^2 s^{-1}]
$D_{k,eff}$	effective Knudsen diffusion coefficient [m^2 s^{-1}]
E_s	activation energy [kJ kg^{-1}]
f	fluid friction coefficient
G_a	air mass flux, m_G/A [kg m^{-1} s^{-1}]
h_c	convective heat transfer coefficient [kW m^{-2} K^{-1}]
H_{ads}	heat of adsorption [kJ (kg toluene)$^{-1}$]
K_G	gas-side mass transfer coefficient[kg m^{-2} s^{-1}]
L	bed length [m]
Le	overall Lewis number, $h_c/K_G c_{p,e}$
m	mass of activated carbon [kg]
m_l	mass fraction of toluene in toluene–air mixture [kg toluene (kg mixture)$^{-1}$]
m_G	mass flowrate of toluene–air mixture in adsorption [kg s^{-1}]
M	molecular weight [g mole^{-1}]
N	number of numerical elements
Ntu	number of mass transfer units, $K_G pL/m_G$
P_i	partial pressure [Pa or atm]
p	perimeter of bed, A_s/L [m]
r	non-dimensional radial coordinate, radial coordinate/R
R	particle radius [m]
R_T	gas constant [kJ kg^{-1} K^{-1}]
Re	Reynolds number, $2RV/\nu$
t	time [s]
t^*	non-dimensional time, t/τ
T	temperature [°C or K]
T^*	non-dimensional temperature, T/T_{in}
V	inlet air velocity [m s^{-1}]
W	toluene content [kg toluene (kg desiccant)$^{-1}$]
Y	toluene concentration [ppm]
z	non-dimensional axial coordinate, axial coordinate/L.

---

* Corresponding author. Tel.: 00886 4 2205585; fax: 00886 4 2851941; e-mail: g8561208@mail.nchu.edu.tw.

0017-9310/98 $19.00 © 1998 Elsevier Science Ltd. All rights reserved
PII: S0017-9310(98)00047-7

Greek symbols
γ adsorption/desorption mass flowrate ratio
γ_1 $c_{p,l}/c_{p,e}$
γ_2 $c_{p,e}/c_b$
γ_3 $H_{ads}/(c_b T_{in})$
ε porosity
ν dynamic viscosity [$m^2\ s^{-1}$]
ρ density [$kg\ m^{-3}$]
σ non-dimensional length factor, $[3\nu^2 L(1-\varepsilon_b)/8c_{p,e} T_{in} R^3 \varepsilon_b^3]$
τ half cycle time [s]
τ_s surface tortuosity factor.

Subscripts
0 initial
ave averaged value
b bed
e toluene–air mixture
f final
G regeneration
i initial
in inlet
out outlet
p particle
s particle surface.

1. Introduction

Packed-bed systems are widely used in adsorption of water vapour, organic solvent and some toxic gases. Although they have a higher pressure drop than the newly developed honey-comb type rotary wheel system, their low first cost and low maintenance cost are still attractive to some manufacturers. A simple packed-bed system consists of a single column filled with an adsorbent. During operation, the adsorbent needs to be replaced as it becomes saturated with an adsorbate. A packed-bed system for a cyclic operation usually consists of two columns. The two columns are arranged in a periodic-switched operation. While one is for adsorption, the other is for desorption. In order to proceed a cyclic operation, an input heat is required for the regeneration of the adsorbent in desorption mode. Various adsorbents might have a significant deviation on physical adsorption characteristics. Thus, in a packed-bed system, an adequate adsorbent is selected for a specific adsorbate. For example, activated carbon is usually used for adsorption of oil or organic solvent. Silica gel and molecular sieves are used for adsorption of water vapour.

In this work the adsorption of toluene on a granular activated carbon in a packed bed is investigated. Toluene is a very popular solvent used in electronic, chemical and printing industries. But it is also a substance causing severe environmental pollution. Direct adsorption and incineration are two among many approaches being adopted in the control of toluene emission in industry. An activated carbon packed-bed system with a single column is a device for direct adsorption. As a gas mixture containing toluene passes through the column, the toluene is adsorbed by the activated carbon particles. Thus the quality of the effluent is improved. A packed-bed system with two columns in an incineration system basically forms an efficient process to handle toluene–air mixture. As the system operates with a high adsorption/desorption air mass flowrate ratio (as indicated later), the toluene concentration of the mixture for incineration will greatly increase. This also means that the air mass flowrate for incineration is reduced. Thus less fuel is required and less carbon dioxide is produced to bring the toluene–air mixture to a certain reaction temperature.

A review of the works relating to the heat and mass transfer between an adsorbent and an adsorbate is summarized in this paper. Pesaran and Mills [1, 2] studied the moisture transport in a packed-bed system with particular attention to solid-side resistance to moisture difference in adsorbent particles. In the study the dynamic response of a simple adsorption process was considered, yet the cyclic operation of the packed-bed system was not investigated. Part I of the work [1] is a report of an analytical study of the transient response of a thin silica gel packed bed to a step change in inlet air humidity and temperature. Part II of the work [2] contains the results of an experimental work. A comparison between the result of an experimental measurement and that of a theoretical analysis for a thin silica gel packed bed was performed by Clark et al. [3]. The analysis was based on a gas-side controlled heat and mass transfer model which incorporates the solid-side diffusion resistance in a gas-side mass transfer coefficient. In the result a high initial rate of adsorption was predicted. The sorption rate and apparent solid-side diffusivity of water in silica gel was studied by Kruckels [4] and Lu et al. [5]. In both works the surface diffusion is verified to be the most important mechanism for water vapour adsorbed by regular density silica gel. Thus the ordinary diffusion and Knudsen diffusion can be neglected in a theoretical analysis. Schork et al. [6] did a parametric analysis of thermal regeneration of an adsorption bed. The experimental study was performed for the propane/nitrogen system using a fixed bed of activated carbon. In the analysis the mass transfer model with a variable lumped resistance coefficient provides a result with an acceptable match to the experimental data. Recently San et al. [7] did an experiment on the dehumidification ability of a silica gel packed-bed system. The solid-side diffusion resistance model originally developed by Pesaran and Mills [1, 2] was modified by considering a fluid friction effect in the energy balance.

In this work a transient response of a packed bed for the adsorption of toluene from an air stream is investigated. The adsorbent is a granular activated carbon with irregular geometry. The heat and mass transfer in the packed bed is analyzed using the solid-side diffusion resistance model [7]. An experiment is set up and the exit toluene concentration of the packed bed is measured by using a gas chromatographic analyzer. The experimental result is compared to that obtained from a computer analysis. The computer model is also used to analyze the adsorption process of a packed-bed system with two columns in a periodic steady-state operation. The effects of regeneration temperature, cycle operating time and *Ntu* on the removal of toluene are individually discussed.

2. Mathematical model

Pesaran et al. [1] proposed a solid-side resistance model (SSR) for predicting the transient response of the heat and mass transfer in thin silica gel packed beds. The model includes both solid and gas-side resistances in the analysis of the diffusion of water vapour. In the solid-side resistance model [1] the equilibrium condition on the surface of an adsorbent is initially evaluated. The result then provides the information in the analysis of the heat and mass transfer in the pseudo-channels of the packed-bed column [1, 7]. In this work, an isotherm equation [8] for the adsorption of toluene on a granular activated carbon is provided by the manufacturer and the corresponding expression for the heat of adsorption is adopted. The assumptions used in the analysis are summarized as follows: (i) only surface diffusion is considered—the Knudsen diffusion and molecular diffusion are neglected, (ii) toluene is the only substance adsorbed on the activated carbon, (iii) the heat transfer resistance in the solid is negligible, (iv) the adsorbate obeys the ideal gas behaviour, (v) the adsorbent is in a spherical form. Based on the above assumptions and using several defined non-dimensional variables and parameters, the governing equations can be arranged in the following forms [1, 7]:

(i) Mass diffusion in the particle:

$$\frac{\partial W}{\partial t^*}=\frac{1}{r^2}\frac{\partial}{\partial r}\left(r^2D^*\frac{\partial W}{\partial r}\right) \tag{1}$$

initial condition:

$$W(r,z,t^*=0)=W_0(r,z)$$

boundary conditions:

$$\left.\frac{\partial W}{\partial r}\right|_{r=0}=0$$

$$\left.\frac{\partial W}{\partial r}\right|_{r=1}=-Bi_m(m_{1,s}-m_{1,e})$$

where

$$D_{s,eff}=(1.61\times10^{-6}/\tau_s)\cdot\exp\{-E_s/[R_T(T+273.15)]\}$$

(ii) Equilibrium relationship for the toluene–air system:

$$W=\frac{A_0B_0\left[\exp\left(\dfrac{A_1}{R_T(T+273.15)}\right)\right]P_i}{1+B_0\left[\exp\left(\dfrac{B_1}{R_T(T+273.15)}\right)\right]P_i^c}$$

$$A_0=0.155\times10^{-1}\,\text{kg}\,(\text{kg adsorbent})^{-1}\,(\text{Pa})^{1-c} \tag{2}$$

$$A_1=0.519\times10^3\,\text{kg}\,\text{kJ}^{-1},\quad B_0=0.272\times10^{-6}(\text{pa})^{-c}$$

$$B_1=0.440\times10^3\,\text{kJ}\,\text{kg}^{-1},\quad c=0.896$$

where the conversion between P_i and $m_{1,es}$ is through the following equation (ideal gas relationship),

$$m_{1,s}=\frac{3.194P_i}{101325+2.194P_i}$$

(iii) Mass transfer of toluene in the air stream:

$$\frac{\partial m_{1,e}}{\partial z}=Ntu(m_{1,s}-m_{1,e})(1-m_{1,e}) \tag{3}$$

(iv) Energy balance in the air stream:

$$\frac{\partial T_e^*}{\partial z}=Ntu[Le(T_s^*-T_e^*)+(\gamma_1T_s^*-T_e^*)(m_{1,e}-m_{1,s})]+\sigma[fRe^2] \tag{4}$$

boundary condition:

$$T_e^*(z=0,t^*)=1.0$$

(v) Energy balance in the solid:

$$\frac{\partial T_s^*}{\partial t^*}=\frac{Ntu}{C^*}[Le\cdot\gamma_2(T_e^*-T_s^*)-\gamma_3(m_{1,s}-m_{1,e})] \tag{5}$$

initial condition:

$$T_s^*(z,t^*=0)=T_0/T_{in}$$

where

$$H_{ads}=4.184\times(11418.35+13323.375W)/M$$

In the above governing equations *Ntu* is the number of transfer units of mass transfer. Similar to that of heat transfer, its value is proportional to mass transfer coefficient, column length, column perimeter and inversely proportional to air mass flowrate. Bi_m is the Biot number of mass diffusion in the particle. Its value increases with the gas-side mass transfer coefficient, K_G [1] and decreases with the effective solid-side surface mass diffusion coefficient, $D_{s,eff}$. The value of the Bi_m indicates the relative importance between the gas-side mass transfer and the solid-side mass diffusion in an adsorption process. A process with a low value of the Bi_m implies that the gas-side mass transfer resistance is much greater than the solid-side mass diffusion resistance. In this case, the mass concentration of the adsorbate in the particle can be assumed to be uniform and consequently the gas-side resistance model can be used in the analysis. On the other hand, for a process with a high value of the Bi_m the solid-side mass diffusion resistance is much greater than the gas-side mass transfer resistance. Without considering the mass concentration gradient of the adsorbate in the particle might cause a significant overestimate of the amount of the adsorbate adsorbed by the adsorbent in the adsorption process. Thus in this case, the solid-side resistance model is necessary to be selected in the analysis.

In eqn (1) $D_{s,eff}$ is the effective surface diffusion coefficient; τ_s is the tortuosity factor; E_s is the activation energy. Sladek et al. [9] proposed that the activation energy, E_s, can be approximated as 45% of the heat of adsorption for non-polar adsorbates. Thus once the heat of adsorption is evaluated and the tortuosity factor is selected, the effective surface diffusion coefficient is determined. Equation (2) represents the equilibrium relationship between the activated carbon and toluene (Fig. 1). The equation is in a form of the Redlich–Peterson isotherm [6]. In eqn (2) $m_{1,s}$ is the mass ratio of toluene to toluene–air mixture. Assuming both the toluene and air are ideal gases, the conversion between P_i and $m_{1,s}$ is established. The last term, $\sigma(fRe^2)$, in eqn (4) attributes to the fluid friction effect in the bed. The fluid friction term was verified [7] to be important only when the value of the Reynolds number or the Ntu is large. In the present work, a moderate range of the Reynolds number and Ntu is considered, the effect of the non-dimensional length factor on the adsorption will be negligible. Thus in the analysis the value of $[\sigma(fRe^2)]$ is set to be zero. In eqn (5) C^* can be analog to the capacity rate ratio in heat exchanger theory. If so, $(\rho_b AL/\tau)$ will be viewed as the column capacity rate and m_G will be the flow-stream capacity rate.

Equations (1)–(5) are the governing equations for the heat and mass transfer. The five unknowns are W, $m_{1,s}$, $m_{1,e}$, T_e^* and T_s^*. Equation (1) is solved using a Crank–Nicolson scheme, the other eqns are solved using a fourth-order Runge–Kutta scheme. The values of c_b and W_{ave} are integrated using a composite Simpson's scheme. In the analysis the value of W_{ave} is used to evaluate the heat of adsorption and c_b.

2.1. Transfer coefficients and specific heats

The gas-side heat and mass transfer coefficients adopted in this work were suggested by Pesaran et al. [1] as follows:

$$K_G = 1.7G_a Re^{-0.42} \tag{6}$$

$$h_c = 1.6G_a Re^{-0.42} c_{p,e} \tag{7}$$

The gas-side mass transfer coefficient in eqn (6) was developed from experimental data [1] with the Reynolds number in the range of 10–400. The gas-side heat transfer coefficient in equation (7) was estimated from the gas-side mass transfer coefficient by using the Colburn analogy.

Another set of the gas-side heat and mass transfer coefficients, suggested by Hougen and Marshall [10], also has been substituted into the computer model in this work. The set of transfer coefficients was based on the experimental data done by Ahlberg [11]. The result of the analysis is compared to that obtained by using eqns (6) and (7). The set of the transfer coefficients is represented as follows:

$$K_G = 0.704G_a Re^{-0.51} \tag{8}$$

$$h_c = 0.683G_a Re^{-0.51} c_{p,e} \tag{9}$$

Equation (8) was correlated from a set of experimental data for the adsorption of water vapour from air by a granular silica gel with different mesh sizes. The range of the Reynolds number in the experiment is between 38 and 438. Similar to eqn (7), eqn (9) was obtained from eqn (8) by using the Colburn analogy.

The specific heats of the toluene–air mixture and activated carbon are individually specified as follows:

$$c_{p,e} = 1.2753m_{1,e} + 1.004(1-m_{1,e}) \tag{10}$$

$$c_b = 1.84096W_{ave} + 1.05 \tag{11}$$

In the above equations, the units of h_c and K_G are respectively kW m^{-2} K^{-1} and kg m^{-2} s^{-1}, the unit of the specific heat is kJ kg^{-1} K^{-1}. In eqn (10) the constant pressure specific heat of toluene in vapour phase is 1.2753 kJ kg^{-1} K^{-1} and that of air is 1.004 kJ kg^{-1} K^{-1}. In eqn (11) the specific heat of the activated carbon is 1.05 kJ kg^{-1} K^{-1} and that of toluene in adsorbed phase is 1.84096 kJ kg^{-1} K^{-1}.

2.2. Comparison of molecular and Knudsen diffusion fluxes with surface diffusion flux

In the derivation of eqn (1), the Knudsen and molecular diffusion fluxes are assumed to be much smaller than the surface diffusion flux. The surface diffusion thus remains the only mechanism governing the diffusion flux in the particle. In the following, the validity of this assumption is carefully examined.

The molecular diffusion coefficient for the toluene–air mixture is evaluated by using the empirical correlations of Fuller et al. [12, 13]. The Knudsen diffusion coefficient is evaluated by using the result of kinetic theory for the diffusion of a molecule in a straight cylindrical pore [14]. At 40°C, the former is 8.86×10^{-6} m^2 s^{-1} and the latter is 3.04×10^{-7} m^2 s^{-1}. In the evaluation of the Knudsen diffusion coefficient, the average pore diameter of the activated carbon is considered to be 17 Angströms. The above calculated values give a ratio of Knudsen diffusion coefficient to molecular diffusion coefficient of 3.5%. Thus the molecular diffusion is negligible as compared to the Knudsen diffusion [14]. Several other cases with the temperature between 30°C and 100°C are also checked and the conclusion is the same.

In order to obtain the form of eqn (1), two non-dimensional groups, $[\partial(\rho m_1)/\partial W]/\rho_P$ and $(D_{K,\mathrm{eff}}/D_{S,\mathrm{eff}})[\partial(\rho m_1)/\partial W]$, also must be much smaller than unity [1]. The partial derivative in the former can be obtained directly by evaluating the slope of the adsorption isotherms. At 40°C, it is evaluated to be less than 3.15×10^{-5}. The magnitude of the latter actually indicates the relative importance between the Knudsen diffusion and the surface diffusion. The value is evaluated to be less than $0.046\varepsilon_p$. ε_p is the particle porosity which is less than unity. Thus the Knudsen diffusion flux is much smaller than the surface diffusion flux. For other temperatures in the considered process, the above conclusion also has been checked and found to be correct.

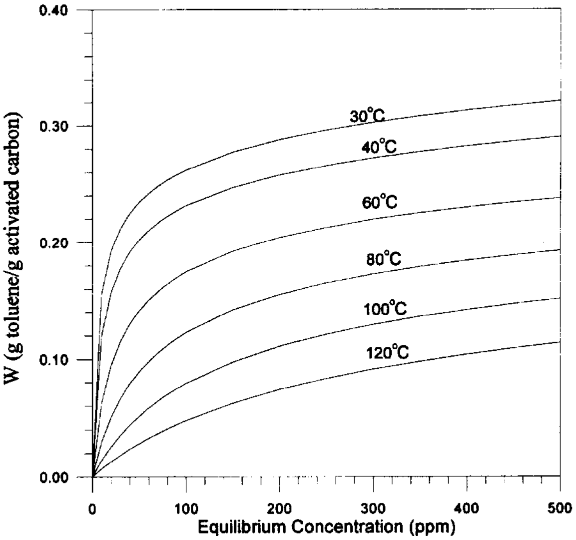

Fig. 1. Adsorption isotherms.

3. Experimental set-up and procedure

In this work an experimental measurement for the adsorption of toluene from air by the granular activated carbon in a packed bed is performed. The shape of the activated carbon is irregular and the thickness of the activated carbon layer in the bed is 30 mm. The porosity of the bed is 0.3. In order to obtain an average adsorption characteristics of the activated carbon, the diameter of the packed bed needs to be large enough to reduce the uncertainty of the air distribution in the bed. In this work the diameter of the packed bed is 250 mm. Since a long operating time period and a large diameter of the packed bed are considered, a specially designed testing system is adopted. The experimental set-up is shown in Fig. 2 which mainly includes a toluene vapourization system, a packed-bed system and a gas chromatographic analyzer (PHOTOVAC-10S50). The experiment is conducted in a space with dimension of 4.6 × 3.6 × 3.5 m (length × width × height). The room temperature is controlled at 31°C with a maximum deviation of 1.0°C.

The toluene vapourization system is also shown in Fig. 2. An open cylindrical container with diameter of 120 mm and height of 100 mm filled with toluene is placed in a water bath. The water temperature is maintained at 34 ± 0.2°C with a PID controller. The isothermal condition of the water bath allows the toluene to have a constant evaporation rate during the entire testing period. In order to reach a uniform toluene concentration in the measuring space, several fans are used to recirculate the air. As the blower in the outdoor operates, eventually the toluene concentration in the measuring space approaches to an equilibrium condition. The 1 hp centrifugal blower in Fig. 2 is controlled by a programmable controller which allows the blower to be operated at an appropriate rotational speed. In this work the inlet air velocity of the packed bed is controlled at 0.78 m/s. In doing so, the toluene concentration at the inlet of the bed is 47.5 ppm with a 10% maximum variation.

Since the shape of the activated carbon particles is irregular, a proposed equivalent diameter is used in the computer modeling. Five thousand particles are counted and selected to be the sample. By measuring the mass of the particles and dividing by the particle density, the volume of the five thousand particles is evaluated. Assuming all the particles are in the same spherical size, the equivalent diameter of the activated carbon particles is obtained. In this work the equivalent diameter is evaluated to be 2.42 mm.

In the beginning of the experiment the temperature of the water bath and the room air individually is set up in the designated range. After adding toluene to the container, the blower is started and draws the mixture (air and toluene) from the space. During the operation a certain amount of fresh air flows into the room through a small hole to balance the outlet exhaust toluene–air mixture. The process proceeds continuously for 16 h. After that, several measurements are performed to insure that the room toluene concentration is under a steady state condition. At this moment, the used packed bed in the process is immediately replaced by a geometrically similar packed bed. In the new packed bed the amount of the activated carbon is the same as that in the replaced one, however there is no toluene content initially in the fresh activated carbon particles. Every forty minutes the exhaust gas mixture from the blower is sampled and measured using the GC analyzer for the toluene concentration. Throughout the experiment, every hour the toluene–air mixture at the inlet of the bed is sampled and

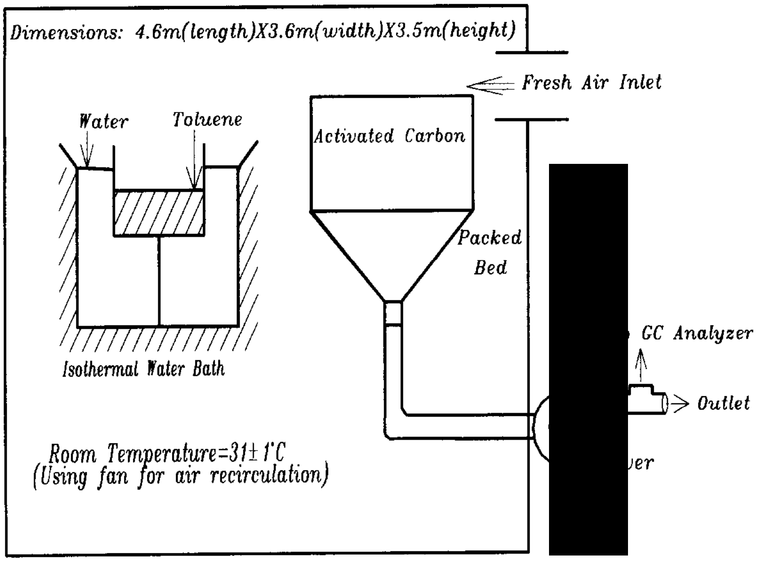

Fig. 2. Experimental set-up.

the consistency of the toluene concentration is checked. The measuring continues for 15 h until the activated carbon is nearly saturated.

4. Results

Figure 3 shows the importance of the number of numerical elements on the simulation result. A tortuosity factor of 4.0, which is an estimated value for the micropores [15], is assumed. The tortuosity factor, τ_s, counts the effect of the varying of diffusion direction and varying of pore cross section on the diffusion flux. A higher value of the tortuosity factor is generally encountered with adsorbents having a lower particle porosity. As shown in the diagram five different numerical grids are selected in the analysis and the corresponding results of the five test runs are represented by the solid lines. By examining the convergency of the results, the numerical elements of the particle and packed bed individually suggested values greater than 40 and 100 respectively. This suggestion also is verified in Table 1. Table 1 shows the mass balance of the toluene in the air and activated carbon. For test run 1 and 2, the number of the numerical elements is not sufficient. Thus the mass of toluene gained in the packed bed is much less than that lost in the air. The circles in Fig. 3 represent the experimental result, which is based on the same operating condition as that in the computer simulations. As can be seen, the initial exhaust toluene

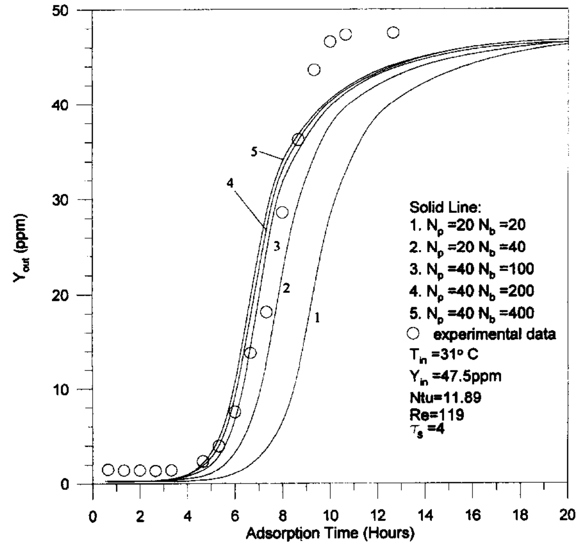

Fig. 3. Effect of number of numerical elements on simulation result.

Table 1
Influence of number of numerical elements on mass balance of toluene

Case	Mass gained in particles $(W_f - W_i)m$	Mass loss in air stream $[\int(Y_{in} - Y_{out})\,dt]m_G$
1	184.038	263.44
2	186.188	227.03
3	200.328	208.79
4	200.63	203.12
5	200.78	201.05

Unit: grams.

concentration in the experiment is maintained at 1 ppm for 4 h. Then the breakthrough phenomenon causes the exhaust toluene concentration abruptly to increase until the activated carbon in the packed bed is saturated. A significant deviation between the experimental data and computer result occurs at the beginning of the process and at the moment the activated carbon to be saturated. The cause of the deviation could be due to the conversion of the activated carbon particles from an irregular shape into a spherical geometry in the computer simulation. For an irregular shape adsorbent, the air distribution in the packed bed would be non-uniform. Thus part of the toluene–air mixture leaves the packed bed without having enough contact with the adsorbent. This might cause the exit toluene concentration to appear to be higher at the beginning of the measurement. Also, the conversion of the particle size from an irregular shape into a spherical geometry is based on the fact that both have the same mass rather than surface area. The thickness of the irregular activated carbon particle is actually very small. Thus, the internal diffusion length of the real particle is much smaller than that of the assumed spherical particle. Moreover, the surface area of the former is greater than the latter. Therefore the particle in the experiment appears to reach the saturation condition earlier than that in the computer simulation.

The simulation result in Fig. 3 is based on the tortuosity factor of the activated carbon with a value of 4.0. In Fig. 4 the effect of the tortuosity factor on the simulation result is investigated. In the analysis the tortuosity factor is individually considered as 1, 2, 4 and 6. The value of the tortuosity factor of 1.0 means the path of the micropores in the activated carbon is straight. The higher the value of the tortuosity, the higher the internal resistance of the toluene diffusion inside the particle. As the activated carbon approaching to be saturated, the simulation result with the tortuosity factor of 1.0 appears to have a good match with the experimental data. To have a lower value of the tortuosity factor in the simulation means to enlarge the internal diffusion of toluene in the particle. Thus the saturation of the activated carbon will be preceded. As explained earlier, the conversion of the particle from an irregular shape into a spherical geometry causes a slower internal diffusion in the simulation than that in the experiment. Thus the adoption of the tortuosity factor with the value of 1.0 corrects the above deficiency.

Figure 5 shows the comparison of the numerical result, using the Ahlberg's heat and mass transfer coefficients, with that obtained from the experimental measurement. Similar to the analysis in Fig. 4, four different tortuosity factors are individually considered in the numerical simulation. The Ahlberg's heat and mass transfer coefficients [9] is much smaller than that suggested by Pesaran [1]. Thus in Fig. 5 the initial exit toluene concentration of the simulation result is much greater than that in Fig. 4. Also, the time period to reach the saturation condition in the former is longer than that in the latter. As shown in Fig. 4, all the four numerical results match poorly with the experimental data. Thus the Ahlberg's heat and mass transfer coefficients are not recommended for use in the simulation model, for the adsorption of toluene from air by the activated carbon in the packed bed system.

Figures 6–10 are the simulation results of the packed bed system in a periodic steady-state counterflow operation. In the figures the parameter, C^*, is replaced by the

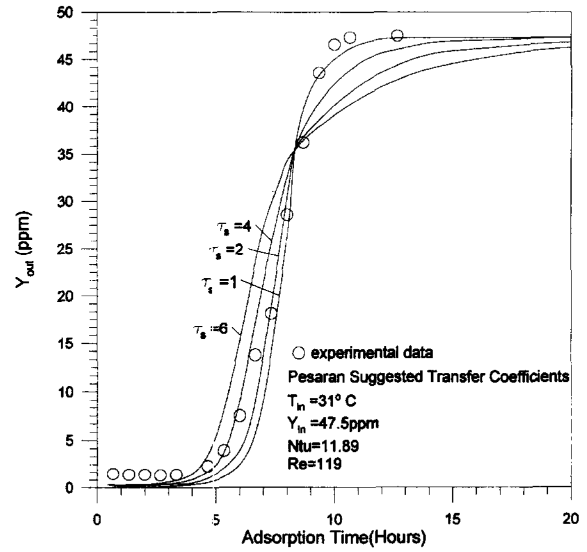

Fig. 4. Effect of tortuosity on simulation result (Pesaran suggested heat and mass transfer coefficients).

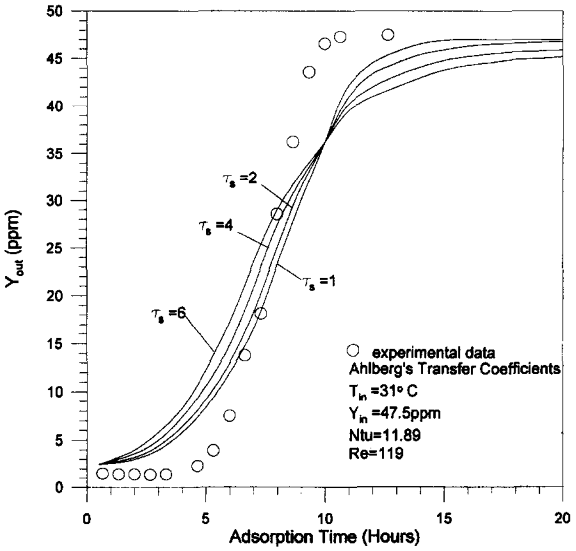

Fig. 5. Comparison of simulation result (Ahlberg's heat and mass transfer coefficients) with experimental data.

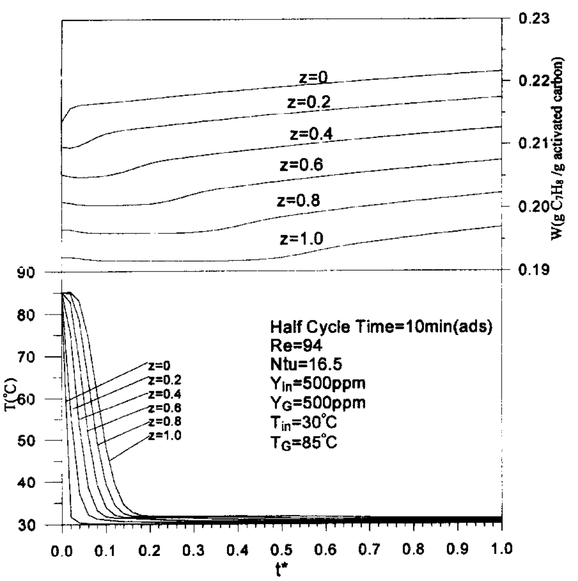

Fig. 6. Variation of bed temperature and toluene content in adsorption mode.

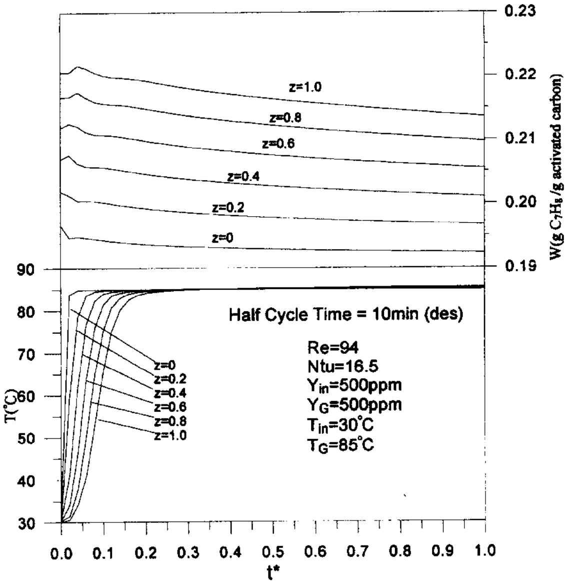

Fig. 7. Variation of bed temperature and toluene content in desorption mode.

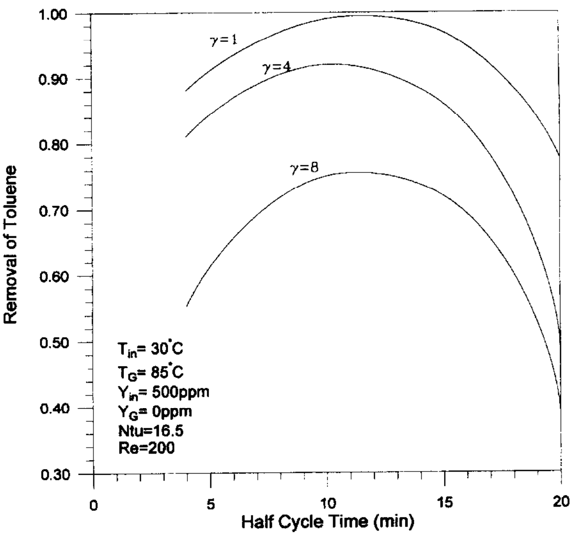

Fig. 8. Effect of adsorption/desorption mass flowrate ratio on removal (85°C regeneration).

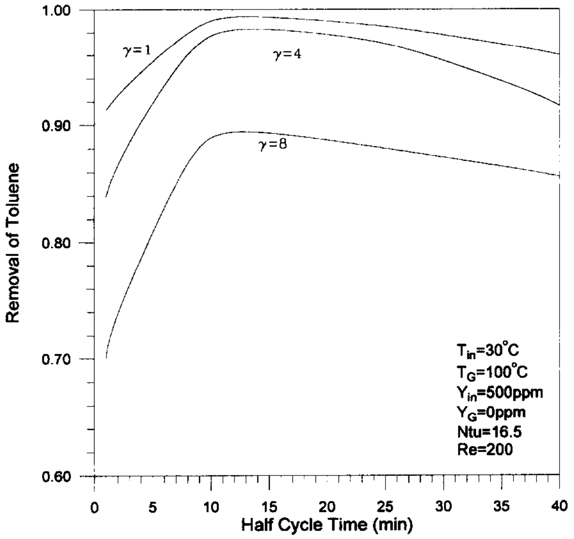

Fig. 9. Effect of adsorption/desorption mass flowrate ratio on removal (100°C regeneration).

half cycle time, τ. The conversion from C^* to τ is through the following relationship: $\tau = (R\rho_p/3K_G)(Ntu/C^*)$. In the present analysis the size of the activated carbon is fixed. Once the value of the Re is selected, the inlet air velocity of the bed can be calculated. The calculated inlet air velocity and the Reynolds number are used to evaluate the value of K_G. Using the above equation, the value of C^* can be converted into τ. Figures 6 and 7 show the variation of the bed temperature and toluene content individually in the adsorption and desorption modes for a specific operating condition. In Figs 6 and 7 the inlet of the bed for each mode is specified by $z = 0$ and the outlet is $z = 1.0$. The result shows that the bed temperature reaches a thermally equilibrium condition before the fraction of the half cycle time, t^*, less than 0.2. Figure 6 also shows that the toluene content of the activated carbon in the inner layer initially decreases. As the corresponding bed temperature drops down, the activated carbon starts to adsorb toluene from the tolu-

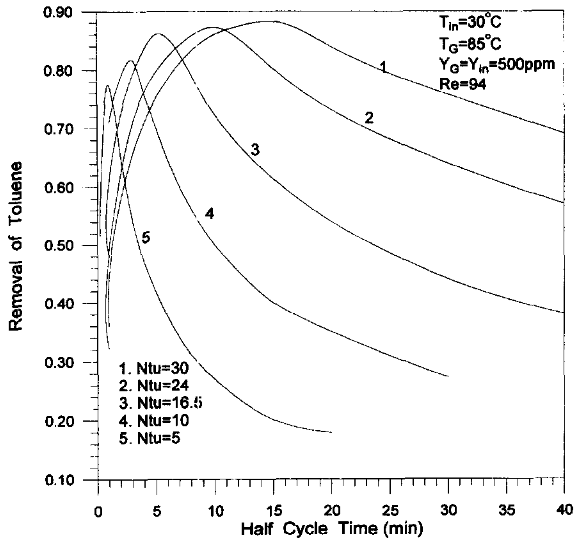

Fig. 10. Effect of *Ntu* on removal of toluene.

ene–air mixture. Figure 7 shows that the entire bed temperature in the desorption mode reaches the regeneration temperature before the fraction of half cycle time, t^* of 0.2. The toluene content of the activated carbon in the inner layer initially increases. For a short period of time, as the corresponding bed temperature rises, the activated carbon starts to desorb.

Figure 8 shows the effect of adsorption/desorption mass flowrate ratio on the removal of toluene for the case with the regeneration temperature of 85°C. The removal of toluene is defined as the average change of the toluene concentration between the inlet and outlet of the bed divided by the inlet toluene concentration. As shown in the result, for every adsorption/desorption mass flowrate ratio there exists an optimum half cycle time and its corresponding maximum removal of toluene. As expected, the maximum removal of toluene decreases as the value of the mass flowrate ratio increases. However the corresponding half cycle time does not vary significantly. In the result it shows that the maximum removal of toluene almost reaches 1.0 for the case with the mass flowrate ratio of 1.0. But it also shows, for the case with the mass flowrate ratio of 8.0, the maximum removal of toluene is only 0.75. Figure 9 represents the effect of adsorption/desorption mass flowrate ratio on the removal of toluene for the case with the regeneration temperature of 100°C. The result in Fig. 9 appears to be similar to that in Fig. 8. For the case with the mass flowrate ratio of 8.0, the corresponding maximum removal of toluene is 0.89. Hence for the operation with a higher value of the mass flowrate ratio, a higher regeneration temperature should be used to achieve a higher removal of toluene.

Figure 10 shows the effect of the *Ntu* on the removal of toluene for the packed-bed system. The result reveals that the maximum removal of toluene increases with the *Ntu*. But as the value of the *Ntu* reaches 16.5, a further increase of the value of the *Ntu* does not result in a significant increase of the removal of toluene. The increase of the value of the *Ntu* can be viewed as an increase of the depth of the bed. Thus as the value of the *Ntu* increases, the total heat and mass transfer area in the bed will increase. This results in an upgrade of the removal of toluene. Figure 10 also shows that the corresponding optimum half cycle time increases as the value of *Ntu* increases. For a system with a longer bed, more desorption time period will be needed to regenerate the activated carbon in the bed. Thus the optimum half cycle time increases as the value of the *Ntu* increases.

5. Conclusions

The process of toluene adsorbed on an irregular shape activated carbon particle in a packed bed is analyzed using the solid-side resistance model. The selected number of numerical grid points has a significant effect on the accuracy of the simulation result. For the analysis with the tortuosity factor of 4.0, at the beginning of the process and at the moment as the activated carbon approaching saturation, the deviations between the simulation result and experimental data are evident. The deviations are individually attributed to the non-uniformity of the flow in the bed and the deficiency of the model in the conversion of the particles from an irregular shape into an ideal spherical geometry. For the analysis with the tortuosity factor of 1.0, the latter deviation is minimized. In the work it also has verified that the Pesaran suggested heat and mass transfer coefficients yields a more accurate simulation result than that using the Ahlberg's heat and mass transfer coefficients.

The time period for the toluene–air mixture and all the activated carbon in the packed bed to reach a thermal equilibrium can be within 0.2 of the half cycle time. Before reaching the thermally equilibrium condition, the adsorption ability of the activated carbon is poor. In operation with the value of the adsorption/desorption mass flowrate ratio of 4.0, the packed-bed system can still achieve a removal of toluene over 0.9. Thus, the system is an efficient and effective device to handle toluene emission. For the operation with a high adsorption-/desorption mass flowrate ratio, a rise of the regeneration temperature will be the most effective way to upgrade the adsorption ability of the packed bed. The removal of toluene increases with the value of the *Ntu*. The corresponding optimum half cycle time for the maximum removal of toluene also increases with the *Ntu*. However, for the value of the *Ntu* greater than 16.5, the increasing rate slows down.

References

[1] Pesaran AA, Mills AF. Moisture transport in silica gel packed beds—I. International Journal of Heat and Mass Transfer 1987;30:1037–49.

[2] Pesaran AA, Mills AF. Moisture transport in silica gel packed beds—II. International Journal of Heat and Mass Transfer 1987;30:1051–60.

[3] Clark JE, Mills AF, Buckberg H. Design and testing of thin adiabatic desiccant beds for solar air conditioning applications. Journal of Solar Energy Engineering 1982;103:89–91.

[4] Kruckels WW. On gradient dependent diffusivity. Chemical Engineering Science 1973;28:1565–76.

[5] Lu, LT, Charoensupaya D, Lavan Z. Determination of sorption rate and apparent solid-side diffusivity of pure H_2O in silica gel using a constant volume/variable pressure apparatus. Journal of Solar Energy Engineering 1991;113:257–63.

[6] Schork JM, Fair JR. Parametric analysis of thermal regeneration adsorption beds. Industrial and Engineering Chemistry Research 1988;27:457–69.

[7] San JY, Jiang GD. Modeling and testing of a silica gel packed-bed system. International Journal of Heat and Mass Transfer 1994;37:1173–9.

[8] Lian, CS. Computer simulation and performance analysis of a rotary adsorption wheel. MS Thesis. Department of Chemical Engineering, Feng Chia University, Taiwan, 1993.

[9] Sladek KJ, Gilliland ER, Baddour RF. Diffusion on surfaces. II. Correlation of diffusivities of physically and chemically adsorbed species. Industrial and Engineering Chemistry: Fundamentals 1974;13:100–5.

[10] Hougen OA, Marshall WR, Jr Adsorption from a fluid stream flowing through a stationary granular bed. Chemical Engineering Progress 1947;43:197–208.

[11] Ahlberg JE. Rates of water vapor adsorption for air by silica gel. Industrial and Engineering Chemistry 1939;31:988–92.

[12] Fuller EN, Schettler PD, Giddings JC. A new method for prediction of binary gas-phase diffusion coefficients. Industrial and Engineering Chemistry 1966;58:19–27.

[13] Sherwood, TK, Pigford RL and Wilke CR. Mass Transfer. New York: McGraw-Hill, 1975.

[14] Karger J, Ruthven DM. Diffusion in Zeolites and Other Microporous Solids. New York: Wiley, 1992.

[15] Scatterfield CN. Heterogeneous Catalysis in Practice. New York: McGraw-Hill, 1980.